Electronic Supporting Information (ESI) for

Water-redispersible and high-yield *α*-chitin nanocrystals isolated using electron-beam irradiation for adsorbents to remove heavy metals and dye†

Hyunho Lee,[a,b] Min Haeng Heo,[a,b] Haemin Jeong,[a,b] Se Young Kim,[a,b] Jeong Suk Yuk,[a] Sae Hume Park,*[a] and Jihoon Shin*[a,b]

[a]Center for Environment & Sustainable Resources, Korea Research Institute of Chemical Technology (KRICT), 141 Gajeong-ro, Yuseong-gu, Daejeon, 34114, Korea.

E-mail: tpark@krict.re.kr, jshin@krict.re.kr

[b]Department of Advanced Materials & Chemical Engineering, University of Science & Technology (UST), 217 Gajeong-ro, Yuseong-gu, Daejeon, 34113, Korea.

†Electronic supplementary information (ESI) available. See DOI:

*Corresponding authors e-mail: tpark@krict.re.kr; jshin@krict.re.kr

Supporting Information consists of six figures over fourteen pages.

Annexure S1

Experimental

Materials

A commercial α-chitin powder from shrimp shell (practical grade, Sigma-Aldrich, USA) was used as the starting material, with a deacetylation degree (DD) of 6.5%, as determined by both FT-IR and solid state ^{13}C CP-MAS NMR spectroscopies. Sodium hydroxide solution (1M), hydrochloric acid solution (3M), and sodium bromide (99%) were purchased from DAEJUNG CHEMICALS & METALS (Korea). 2,2,6,6-tetramethylpiperidine-1-oxyl (TEMPO, J&H CHEM, China) and Sodium hypochlorite solution (8%, JUNSEI Chemical, Japan) were used as received without further purification as the oxidizing agents to prepare TEMPO-oxidized chitin nanocrystals (ChNC-TO). Adsorption reagents including copper(II) nitrate trihydrate (puriss. p.a., 99−104%), iron(III) nitrate nonahydrate (≥98%), Ponceau S (dye content, 75%), and Toluidine blue O (dye content, 80%) were purchased from Sigma-Aldrich.

Characterizations

The values of weight-averaged molar masses ($M_{w,SEC}$) and the polydispersity index ($Đ$) of the disassociated chitins were determined with a size exclusion chromatography (SEC, FUTECS SD-500) system equipped with a refractive index detector in LiCl/DMAc (0.9 wt %) at 40 °C relative to poly(styrene) standards.[S1] The freeze-dried disassociated chitin samples were dissolved in LiCl/DMAc (9 wt %) by vigorous stirring at room temperature. They were diluted to 0.9 wt % by adding pure DMAc and subsequently filtered through a hydrophobic poly(tetrafluoroethylene) (PTFE) Millipore Membrane with a 0.22 μm pore size. The samples were passed through three WAT034124 Shodex KD-806M columns (10 μm, 8 mm × 300 mm) at 40 °C under a constant flow rate of 1 mL min^{-1}. The resulting $M_{w,SEC}$ values were used to determine the degree of polymerization (DP$_w$), considering the portions of N-acetylglucosamine and D-glucosamine units in the chitins.

The effect of EBI on the structure of the α-chitin was investigated by Fourier transform infrared spectroscopy (Cary 630 FT-IR, Agilent Technologies, USA) from 4000 to 400 cm^{-1}. The sample

pellets for FT-IR analysis were obtained by mixing and pressing KBr powder (150 mg) with the freeze-dried chitin samples (4 mg). The ratios of the absorption intensities for the amide II band and C−O stretching vibration (A_{1560}/A_{1030}) were calculated to determine the degree of deacetylation (DD) of the disassociated chitins according to the previous study.[S2]

Solid-state ^{13}C cross polarization-magic angle spinning NMR (^{13}C CP-MAS NMR) was also performed to obtain the integration ratios of C8 to C1 peak (I_{C8}/I_{C1}), as reported in previous studies.[9] The ^{13}C cross-polarization spectra were obtained on an Agilent DD2 400 spectrometer operating at a Larmor frequency of 400.25 MHz for ^{1}H and 100.64 MHz for ^{13}C. The spectra were obtained at room temperature using a 100 kHz proton dipolar decoupling field, matched cross-polarization (CP) fields of 50 kHz, a proton 90° pulse of 2.5 μs, and magic angle spinning (MAS) at a spinning rate of 20 kHz. The acquisition time was 0.15 s and an average number of 4096 scans were acquired for each spectrum. The degree of deacetylation (DD) of the EB irradiated chitins was calculated by both the A_{1560}/A_{1030} from FT-IR spectroscopy and I_{C8}/I_{C1} from the ^{13}C CP-MAS NMR analysis, respectively.

The carboxylate contents (mmol g^{-1} chitin) of the freeze-dried samples including Ch-E series and Ch-TO were calculated by conductometric titration method using a high-end titrator (888 Titrando, Metrohm AG, Switzerland).[S3] The freeze-dried chitin samples (0.1 g) were added to deionized water (60 mL) and the pH values of the samples were adjusted to pH 9 using a small amount of 0.5 M NaOH solution. To prepare a well-dispersed slurry, the mixture was stirred for 30 min. Then, 0.1 M HCl solution was added to the suspension to set the pH value below 3, and then 0.05 M NaOH solution was dropwise added to the mixture at a rate of 0.1 mL min^{-1} up to pH 11. We determined the carboxylate contents by subtracting the amino contents (<1% for Ch-E series and 6.5% for Ch-TO) from the titration curves, and confirmed by the degree of N-acetylation (DA) of the samples obtained from the infrared spectroscopy and solid-state ^{13}C NMR analysis.

The X-ray diffraction (XRD) measurement was carried out with a Rigaku Ultima IV X-Ray diffractometer using Cu radiation ($\lambda = 0.154$ nm) operated at 40 kV and 40 mA, to study the effect of the EBI, TEMPO oxidation, acid hydrolysis, and HPH system on the crystallinities of all the disassociated chitins, chitin nanocrystals (ChNCs), and redispersed ChNCs. The X-ray diffractograms

were acquired at 0.03° sec^{-1} over the scan range: 2θ = 5 to 40°. The crystallinity index (CrI) values of the samples were calculated from the Segal equation: CrI (%) = [(I_{110}–I_{am})/I_{110}] × 100, where I_{110} is the highest intensity of the crystalline plane (110) lattice diffraction in the chitin at a 19.6°, and I_{am} is the intensity of the amorphous reflection at 16.0°.[S3]

The thermal degradation of the freeze-dried chitin samples were observed using a TA Q500 themrogravimetric analyzer under nitrogen gas at a rate of 10 °C min^{-1} from 25 to 500 °C. The transmittance of all the ChNCs and redispersed suspensions (0.1 wt %) were measured by UV-vis spectrometer (Shimadzu, UV-1650PC, Japan) in visible wavelengths ranging from 400 to 600 nm. To study the surface charge of the ChNCs and the redispersed suspensions (0.1 wt %), the zeta-potential values of the nanoparticles were determined using Laser-Dropper-Velocimetry (LDV) (Zetasizer Nano ZS series, Malvern Instruments Ltd, UK). The Tyndall scattering phenomena of the ChNCs and the redispersed suspensions (0.1 wt %) was observed by He−Ne laser (632.8 nm).

The morphologies of the disassociated chitins and the spray-dried ChNCs, and the aerogels obtained after freeze-drying the self-standing hydrogels containing metals and organic dyes, were examined by scanning electron microscopy (SEM) using a MIRA 3 field emission scanning electron microscope (Tescan, Czech Republic) with an acceleration voltage of 20 kV. The metals and dyes absorbed in the aerogels were detected by energy dispersive X-ray spectrometer (EDS, Bruker, Quantax 200, Germany) equipped with FE-SEM. To measure the dimensions of the ChNCs and the redispersed ChNCs, a drop of these suspensions (0.01 wt %) was deposited on a thin-carbon-coated 200 mesh copper grid (CF200−Cu, Electron Microscopy Sciences, USA), and then negatively stained with uranyl acetate solution (2.0% w/v) and allowed to dry. The samples thus prepared were analyzed with a JEM-2100F transmission electron microscope (TEM) operated at an accelerating voltage of 200 kV. The TEM images were taken under diffraction contrast in the bright-field mode without prior contrast enhancement. Rheological tests were performed to measure the mechanical properties (storage modulus (G') and loss modulus (G'')) of the ChNC hydrogels containing heavy metal ions or organic dyes using a MCR 302e rheometer (Anton Parr, Austria) operating in 25 mm parallel-plate and 1 mm

gap distance. The tests were performed at 25 °C. The dynamic frequency sweeps were conducted with oscillatory frequencies between 0.1 and 100 rad/s at 0.1% strain.

Adsorption in redispersed ChNC suspensions

The transparently and homogeneously dispersed ChNC-E1000 (RU) suspension was adjusted to pH 11 by adding 0.5M NaOH solution, to maximize the surface charge density. To investigate the adsorption properties of ChNC-E1000 (RU) in this study and using ChNC-H as a reference, water-soluble salts including cationic heavy metals (copper(II) nitrate trihydrate and iron(III) nitrate nonahydrate) and cationic/anionic dyes (toluidine blue O and Ponceau S) were directly introduced into the suspensions at concentrations of 0.2 mmol mL^{-1} for the metals and 0.5 mg mL^{-1} for the dyes, respectively. Gelation immediately occurred after shaking and vortexing for 2 min. The gel suspensions were centrifuged and washed with deionized water several times, to remove the unabsorbed organic dyes or metal ions and to separate agglomerated ChNC hydrogel. The aggregated hydrogels of ChNC-E1000 (RU)−Cu^{2+}, ChNC-E1000 (RU)−Fe^{3+}, and ChNC-E1000 (RU)−toluidine blue O were collected and showed self-supporting or standing forms. Meanwhile, ChNC-H was used to adsorb anionic dyes such as Ponceau S in acidic conditions (ca. pH 4), under conditions identical to that of ChNC-E1000 (RU). The four kinds of self-standing hydrogels with solid contents of 3−8 wt % were freeze-dried to obtain aerogels. The morphologies of the aerogels were observed by scanning electron microscopy (SEM, MIRA 3, Tescan, Czech Republic) and the metals and dyes adsorbed on the surface of the aerogels were detected using an energy dispersive X-ray spectrometer (EDS, Bruker, QUANTAX 200, Germany).

Adsorption kinetics

To determine adsorption isotherms, the desired amount of coper(II) nitrate trihydrate, iron(III) nitrate nonahydrate, and toluidine blue O (a cationic basic dye) were directly introduced into the 40 mL of ChNC-E1000 (RU) suspensions (0.5 wt %). The mixtures were filtered to obtain the solutions containing the residual cationic heavy metals or dye that did not participate in the suspensions. The

filtration was carried out using a membrane filter (PTFE, 0.1 μm pore size), which had little effect on the concentrations of the substrates after vortexing the mixtures for 2 minutes at room temperature. The quantities of the heavy metal and dye cations absorbed on ChNC-E1000 (RU) were determined by measuring the absorbances of the solutions obtained after filtration using a UV-Vis spectrometer at $\lambda = 304$ nm for Cu^{2+} and Fe^{3+}, and $\lambda = 590$ nm for toluidine blue O (Shimadzu, UV-1650PC, Japan). To prevent interference from extracted ChNC particles after filtration, the filtered ChNC-E1000 (RU) solution without adding the heavy metal cations or dye was used to obtain the baseline. The amounts of Cu^{2+}, Fe^{3+}, and toluidine blue O were then calculated using the absorbance vs the concentration calibration curves. The removal efficiencies of heave metal cations or dye in the mixtures were calculated as follows[S4,S5]:
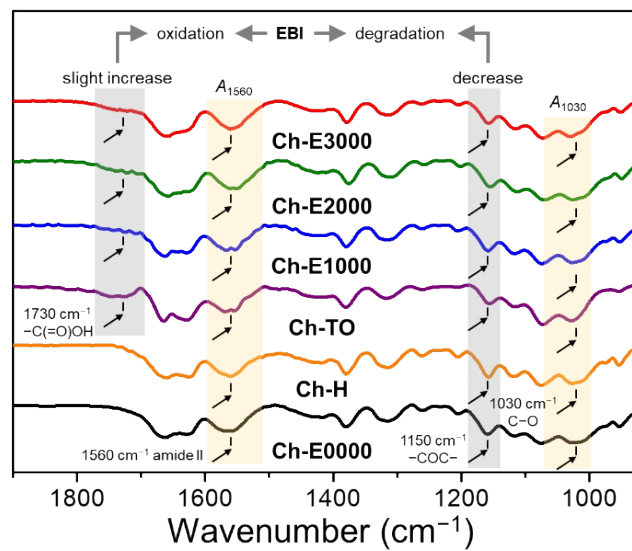
$$\text{Removal efficiency (\%)} = \frac{C_i - C_e}{C_i} \times 100$$

where C_i is the initial concentration (g L^{-1}) and C_e is the equilibrium concentration (g L^{-1}) for the heavy metal cations or dye.
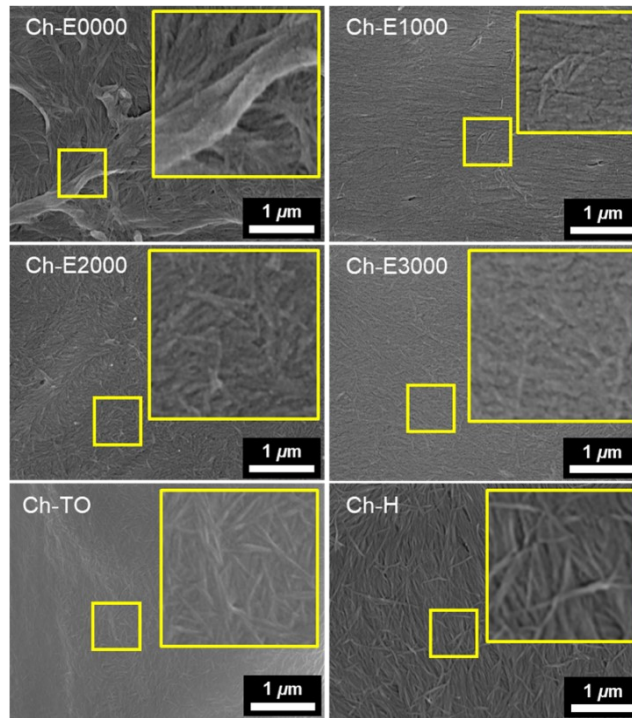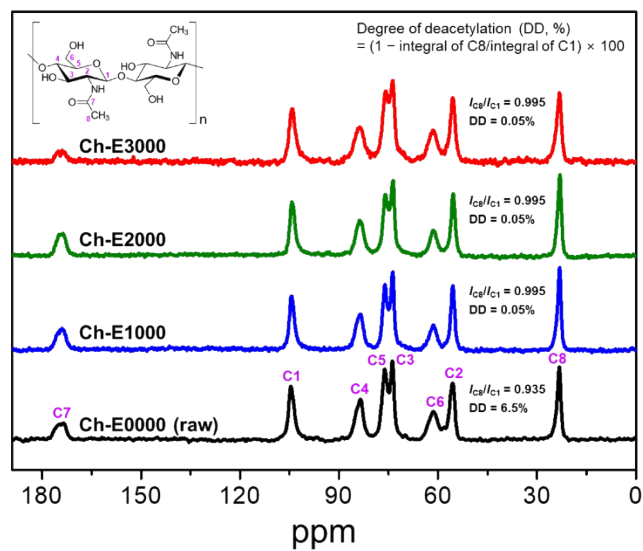
Fig. S1 SEM images of the chitins disassociated by TEMPO-oxidation (Ch-TO), and HCl-hydrolysis (Ch-H), and by electron beam doses of 0 (raw), 1000, 2000, and 3000 kGy (Ch-E series).
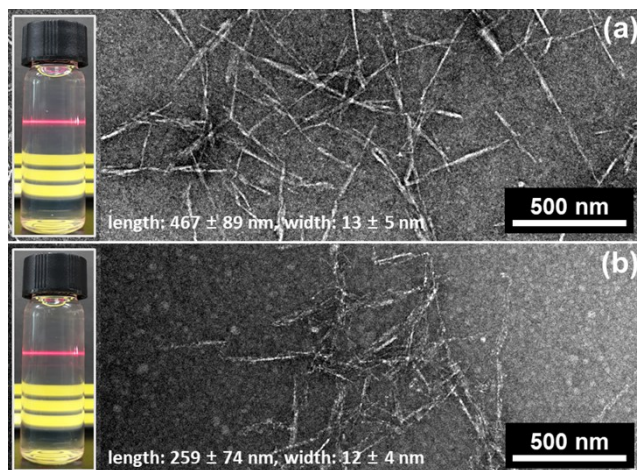
Fig. S2 FT-IR spectra of raw chitin (Ch-E000) and the disassociated chitins obtained after EBI (Ch-E series), HCl-hydrolysis (Ch-H), and TEMPO oxidation (Ch-TO).

Fig. S3 Solid state ^{13}C NMR of EBI-treated chitin series and the degree of deacetylation (DD) values (%) obtained, with the integral C8/C1 ratios of the Ch-E series.

Fig. S4 TEM images of ChNCs disintergrated from chitin dissociated by (a) electron-beam irradiation at (a) 2000 kGy, and (b) 3000 kGy (ChNC-E2000, and ChNC-E3000). Inset: light diffraction with transparency of the aqueous suspension (0.1 wt %) after free settling for six months at room temperature.
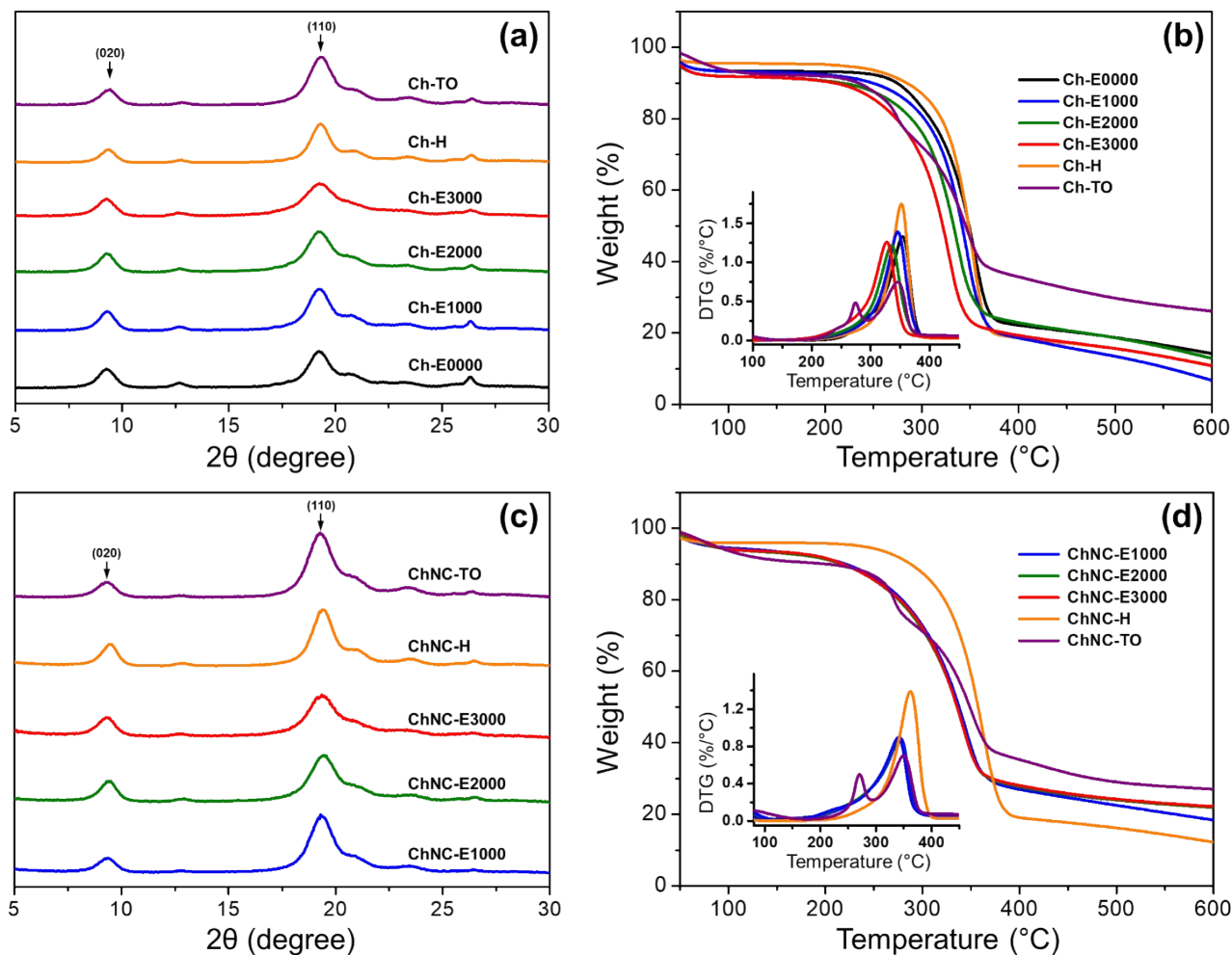
Fig. S5 X-ray diffraction of (a) the disassociated chitins and (c) chitin nanocrystals. TGA thermograms of (b) the disassociated chitins and (d) the chitin nanocrystals. The insets show the DTG curves.
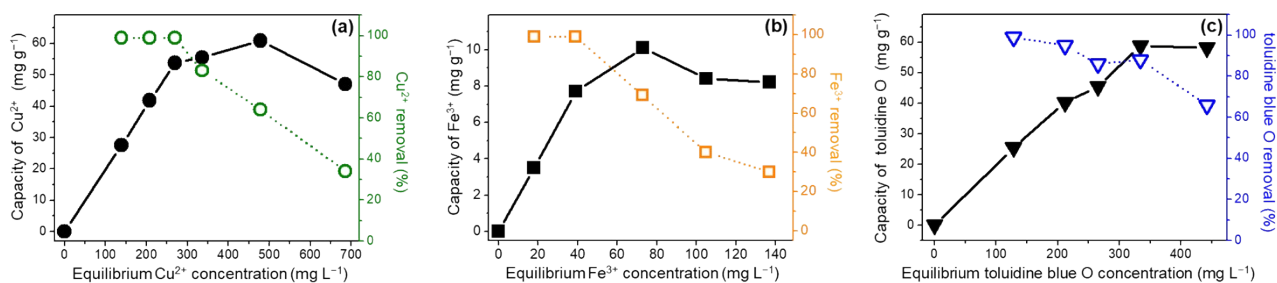
Fig. S6 Adsorption distribution isotherms and the corresponding removal efficiency of (a) Cu^{2+}, (b) Fe^{3+}, and (c) toluidine blue O using the function based on the equilibrium substrate concentrations (adsorbent dosage of 5 g L^{-1} (0.5 wt %) at room temperature and pH 11).

References

(S1) R. Funahashi, Y. Ono, Z.-D. Qi, T. Saito and A. Isogai, *Biomacromolecules*, 2017, **18**, 4357−4363.

(S2) Y. Shigemasa, H. Matsuura, H. Sashiwa and H. Saimoto, *Int. J. Biol. Macromol.*, 1996, **18**, 237−242.

(S3) Y. Fan, T. Saito and A. Isogai, *Biomacromolecules*, 2008, **9**, 192−198.

(S4) Q. Sun, L. -M. Yang, L. Zhang, S. -T. Huang and Z. Xu, *Rare Met.* 2018, **37**, 894−903.

(S5) G. Zhou, J. Luo, C. Liu, L. Chu and J. Crittenden, *Water Research* 2018, **131**, 246−254.